Polymer 51 (2010) 5267–5275

Contents lists available at ScienceDirect

Polymer

journal homepage: www.elsevier.com/locate/polymer

Relaxation of shear-enhanced crystallization in impact-resistant polypropylene copolymer: Insight from morphological evolution upon thermal treatment

Shijie Song, Jiachun Feng*, Peiyi Wu

Key Laboratory of Molecular Engineering of Polymers of Ministry of Education, Department of Macromolecular Science and Laboratory of Advanced Materials, Fudan University, Shanghai 200433, PR China

ARTICLE INFO

Article history:
Received 26 April 2010
Received in revised form
11 August 2010
Accepted 3 September 2010
Available online 15 September 2010

Keywords:
Polypropylene copolymer
Phase morphology
Crystallization

ABSTRACT

Relaxation of shear-enhanced crystallization in an impact-resistant polypropylene copolymer (IPC) upon thermal treatment was systematically investigated, from the sight of phase structure and resultant morphological evolution. Shearing was capable of accelerating the crystallization of IPC, while upon melt annealing, a spontaneous morphological evolution can be observed accompanied by a gradual relaxation of shear-enhanced crystallization. It was found the underlying structural motion during relaxation is in essence a phase separation process towards a multi-layered phase structure, in which crystallizable polyethylene segments are spatially entangled with ethylene-propylene random copolymer chains. The shear-enhanced crystallization originates from the destruction of this multi-layered phase structure which releases crystallizable PE segments to contact the matrix serving as nuclei for the crystallization of polypropylene. Upon annealing, reconstruction of the multi-layered structure can be achieved leading to the relaxation of shear-enhanced crystallization. A conceptual model describing this relationship between phase structure and crystallization behavior in IPC has been proposed.

1. Introduction

As a widely used high-performance polymeric material, impact-resistant polypropylene copolymer (IPC) has drawn considerable interests since its introduction to the market, and the enthusiasm from both industry and academe to this material seems to be expanding in recent years. The appearance of IPC benefits from the application of porous spherical $TiCl_4/MgCl_2$ catalyst and so-called "reactor granule technology", with which made it possible to produce a series of previously unavailable multiphase materials [1]. IPC is commonly produced in-reactor by a multistage polymerization process which involves bulk polymerization of propylene in the first stage and then gas-phased copolymerization of ethylene and propylene in the second stage [1–3]. Recently, a new technique named multi-zone circulating reactor for producing IPC has also been reported [4]. So far, the most concerned topic in the research of IPC is clarifying the origination of its excellent rigidity–toughness balance property. By understanding this structure–property relationship, it will in return enable rational design of IPC materials and optimize their properties through improvements in polymerization and catalyst technology. Earlier studies [5–9] have carried out preliminary compositional characterizations on IPC through different methods. Generally speaking, as an in-reactor alloy, IPC is mainly composed of isotactic polypropylene (iPP) as the matrix component in which ethylene–propylene random copolymers (EPR) are finely dispersed. Besides, some partially crystalline copolymers, either EP block copolymers [9] or so-called EP segmented copolymers [10], with different lengths of polyethylene (PE) or PP segments (EP block copolymers are referred to those copolymers with both crystallizable PE and PP segments, while EP segmented copolymers include crystalline PE or PP segmented polymers, in which only one kind of crystallizable segments exist, either PE segments or PP segments), or even PE homopolymers are proved to exist as well. Through increased understanding of IPC and toughening mechanism, researchers have realized that there exists a gap between the composition and final property, that is how the different components build up entities and distributed in the condensed state (i.e., phase structure and corresponding morphology) [3,11–14]. Therefore, investigations [12–15] on the phase structure and morphology of IPC under different spatial scales have been carried out, from pristine morphology of original particle to microscopically phase separated structure formed in diluted solution. However, a complete understanding of the formation of multi-scale phase structure in IPC as well as its evolution towards the equilibrium state has not been achieved yet.

In a simple approximation, components in IPC can be divided into two categories, the crystalline ones (e.g., iPP, and partially

* Corresponding author. Tel.: +86 21 6564 3735; fax: +86 21 6564 0293.
E-mail address: jcfeng@fudan.edu.cn (J. Feng).

0032-3861/$ – see front matter © 2010 Elsevier Ltd. All rights reserved.
doi:10.1016/j.polymer.2010.09.008

crystalline polymers with long PE or PP segments) and the amorphous ones (i.e., EPR and iPP with very low isotacticity). Thus, both the physical and mechanical property, including rigidity and toughness, of IPC are largely determined by them as well as their mutual interactions. As to the crystalline components, with the contribution and elaborate work of Keller [16–19], Lovinger [20,21], Lotz [22–27] and Bassett [28,29] etc., the properties of semi-crystalline polymers such as PE or PP has been widely studied and discussed. By permanganic etching [28,30–32], directly viewing the fine lamellar structure in bulk PP or PE has also been realized. Hence, the crystallization behavior of simple system containing either iPP or PE has been clarified to a great extent. However, for the system like IPC in which iPP, EPR and other partially crystalline polymers containing PE or PP segments are mixed, the situation becomes complicated. Many factors will influence the crystallization in such complex system, for example, interplay between crystalline components [33,34], interaction between amorphous and crystalline components [35], external thermal and mechanical conditions [36–38], etc. Particularly, the effect of crystalline EP copolymer as interfacial modifiers has made the phase morphology including its evolution under various circumstances a crucial as well as an intriguing topic, which may not only affect the crystallization behavior but also the final performance of the material just as the well-known example of high impact polystyrene [39]. Early studies [40–42] on analogous PP/EPR binary mixtures have already reported that morphological controlling of the blend will result in different crystallization kinetics. During the last decade, Han and Cheng [43–46] have done elaborate studies on investigating the fluctuation-assisted crystallization in binary polyolefin blends to illustrate the relationship between liquid–liquid phase separation and crystallization behavior. Our recent study [47,48] on shear-enhanced crystallization in IPC also suggested that intrinsic phase structure has great influence on the crystallization behavior. In brief, the morphological evolution and the underlying structural changing are extremely important to the understanding of crystallization in multi-component polymer system. However, at least in IPC system, few work has been reported concerning the mentioned topic. Yang [14] et.al have found a spontaneous morphological evolution of processed IPC melt upon thermal treatment, a tendency towards the core-shell phase structure has been observed, nevertheless, no corresponding information about the crystallization has been provided.

In the present study, we reported an experimental study on the relaxation of shear-enhanced crystallization in IPC concerning the morphological evolution and subsequent crystallization behavior. Phase morphologies of pre-sheared IPC samples after different melt annealing procedures were observed using scanning electron microscopy (SEM), and the underlying structural changing was correlated to the relaxation of shear-enhanced crystallization. By solvent fractionation, two characteristic fractions in IPC were separated and each composition, molecular structure, phase morphology as well as the crystallization behavior were characterized. It appears that the different components in the two fractions will be precisely combined and result in a unique multi-layered morphology under equilibrium. Varying this phase structure in IPC may lead to the totally different crystallization kinetics. The possible mechanism describing the phenomenon has been proposed on the basis of experimental data and substantial analysis.

2. Experimental section

2.1. Experimental materials

IPC material used here is a commercial grade in-reactor alloy produced by Qilu Petrochemical Co., SINOPEC (Shandong, China). The weight-average molecular weight was 15.3×10^4 and the polydispersity index was 5.02, as measured by GPC. The ethylene content of IPC was 10.6 wt% as determined by ^{13}C NMR.

2.2. Sample preparation

Both as-received and pre-sheared IPC sample were used for investigation. Pre-shearing process was carried out by a PLE 651 torque rheometer (Brabender, Germany) at a rotor speed of 40 rpm for 10 min under 175 °C with 0.1 wt% anti-oxidant added in. As soon as the melt pre-shearing reached the preset duration, both the rotation and heating of the rheometer were stopped, and then a water-circulation cooling system directly connected to the chamber was opened. The samples left in the chamber were cooled to room temperature by water-circulation and then scratched out for further measurement. Room temperature was kept at 25 °C by air-conditioning, and the pre-sheared sample was denoted as IPC-S. Parameters of the rheometer, the estimated shear rate, and the possible degradation or cross-linking induced by shear process were fully discussed in the Supplementary Material.

Solvent fractionation was performed according to following procedures; First, IPC pellets were dissolved in hot xylene containing 0.1 wt% anti-oxidant and kept for 5 h. The homogeneous solution was then slowly cooled to room temperature. The precipitate was separated by filtration and obtained as fraction Fa. Second, the component dissolved in xylene was washed out by cold methanol and obtained as fraction Fb. Both fractions were dried in vacuum for 24 h before further analysis. The average recovery ratio of solvent fractionation was approximately 95 wt% in which the content of Fa and Fb was about 20 and 75%, respectively.

2.3. Thermal property characterization

A Mettler DSC-1 apparatus was used to analyze the thermal properties. Calibration for the temperature scale was performed using indium ($T_m = 156.60$ °C and $\Delta H_m^0 = 28.45$ J/g) as standard to ensure reliability of the data obtained. The accuracy of measured temperature is ± 0.05 °C. All the experiments were carried out in nitrogen atmosphere. For regular melting and crystallization analysis, the measurements were performed as following procedures: samples were heated to 200 °C and kept for 5 min to erase previous thermal history. Subsequently, samples were cooled to 25 °C at a rate of 10 °C/min, and again heated to 200 °C at a rate of 10 °C/min. The crystallization thermograms were recorded during the first cooling scan, while the melting temperature and fusion enthalpy of the samples were determined during the second heating scan.

2.4. Fourier transform infrared spectroscopy (FTIR)

A Nicolet Nexus 470 Infrared Spectrometer (Thermal Nicolet, America) was used to collect the IR spectra in the region of 4000–500 cm^{-1}. All spectra collected were averages of 64 scans with a resolution of 4 cm^{-1}.

2.5. Wide angle X-ray diffraction (WAXD)

WAXD measurements were performed using a PANalytical X'pert diffractometer (PANalytical, Netherlands) in a reflection mode using Ni-filtered CuKα radiation ($\lambda = 0.154$ nm) under a voltage of 40 kV and a current of 40 mA. Radial scans of intensity versus diffraction angle 2θ were recorded in the region from 10 to 40°.

2.6. Scanning electron microscopy (SEM)

A scanning electron microscopy (TESCAN 5136 MM) was used to observe the sample surface at an operating voltage of 20 kV. Before observation, IPC samples were etched by xylene at room temperature for 5 h and coated with gold.

2.7. Field emission transmission electron microscopy (FETEM)

Thin film samples (thickness < 200 nm) for FETEM observation were prepared by solution casting (0.05 wt%) to a pre-heated copper grids using xylene as the solvent. To erase the influence of dissolving and casting, film samples were further thermally treated before a JEM-2100F (JEOL, Tokyo, Japan) field emission transmission electron microscopy operated at 200 kV was used for observation.

3. Results and discussion

3.1. Thermal properties of as-received IPC and IPC-S

Concerning the complexity of IPC material, a basic understanding of its overall thermal property is necessary. Fig. 1 shows the crystallization and melting curves of as-received IPC and IPC-S samples. In Fig. 1 A, the as-received IPC exists two crystallization peaks (T_p), a major one located at 112.8 °C and another minor one at 89.4 °C indicating the existence of both iPP and crystallizable EP copolymers with different length of PE or PP segments. As for IPC-S sample, it shows remarkable difference in crystallization behavior that the T_p corresponding to iPP component was elevated nearly by 9.0 °C. Our previous crystallization kinetic study on the same IPC material [48] showed that this elevation of T_p could shorten the half-time of crystallization ($t_{1/2}$) by about 1 magnitude during isothermal crystallization at 129.0–135.0 °C. Thus, it points to a shear-enhanced crystallization in IPC, and interestingly this behavior appears to be long-existed reflected on the fact that it will not disappear under normal heating/cooling circles or short-term melt annealing. Subsequent melting behaviors of as-received IPC and IPC-S samples are exhibited in Fig. 1 B. Concerning the low crystallinity of the as-received sample may imply a less perfect crystalline structure, we have checked the possible heating induced melting-recrystallization-remelting process and confirmed that no such process will occur in the as-received samples during heating. The detailed data and discussion can be found in the Supplementary Material. In Fig. 1 B, both samples exhibit two melting peaks. The peak located at higher temperature should be attributed to the melting of iPP component in IPC, and the other one at lower temperature corresponds to the melting of crystalline PE component. For the melting of iPP component, two distinct differences exist between as-received IPC and IPC-S samples. First, peak value was slightly higher for as-received IPC (163.7 °C) than that of IPC-S (162.0 °C). Second, the melting region of as-received IPC was broader than that of IPC-S. The two differences indicate that in IPC-S sample, the iPP molecules preferred to form thinner and more uniform lamellae compared to as-received IPC, which may be related to its faster crystallization kinetic. The weak and broad peaks corresponding to the melting of crystalline PE component were also observed in both samples.

3.2. Relaxation of shear-enhanced crystallization and morphological evolution upon thermal treatment

There are considerable interests to understand the shear-enhanced crystallization in IPC. However, owning to the multi-component and multiphase nature of IPC as stated, interpreting the exact reason behind this interesting phenomenon is still difficult. Based on extensive experimental data, our previous research [47] has suggested a conceptual model to describe the mechanism accounting for this significant shear-enhanced crystallization. In that study, we once observed that the relaxation of enhanced crystallization (i.e., decreasing the crystallization rate backwards) could be achieved through melt annealing, however, no further investigations have been carried out. Obviously, this relaxation behavior is an important breakthrough point from which the internal reason of enhanced crystallization is hopeful to be revealed. Hence, in the present study, we have carried out a comprehensive investigation on the relaxation of shear-enhanced crystallization in IPC during annealing treatment.

Fig. 2 presents the crystallization curves of IPC-S samples after melt annealing at 200 °C for 0–240 min. At this annealing temperature, the influence of oxidant-degradation, cross-linking or other chemical reactions can be excluded with the aid of nitrogen atmosphere and anti-oxidant, as also pointed out by a recent study [49]. In Fig. 2, it shows that T_p of all annealed IPC samples exhibited a recovery tendency towards the as-received IPC sample implying the enhanced crystallization effect was eliminated gradually. Degrees of this recovery showed a dependence of the annealing duration, that is, the longer the annealing performed, the more T_p value was decreased. The minimum annealing time required for the sheared sample to start relaxation at 200 °C is about 15 min which has been discussed in the Supplementary Material. Through annealing for 240 min, T_p have decreased to 114.9 °C. It is no doubt that the shear-enhanced crystallization tends to be completely eliminated with sufficient long annealing. In essence, the underlying structural motion during annealing can be treated as an inverse process of shear-enhanced crystallization. One possible

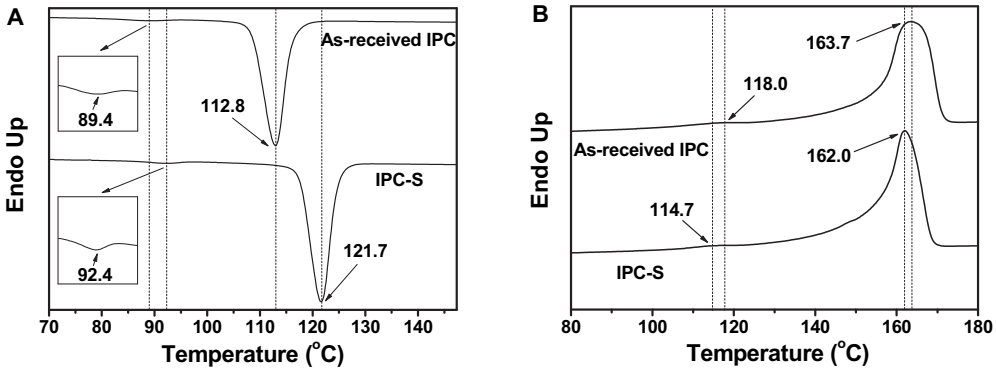

Fig. 1. Crystallization (A) and melting (B) curves of as-received IPC and IPC-S.

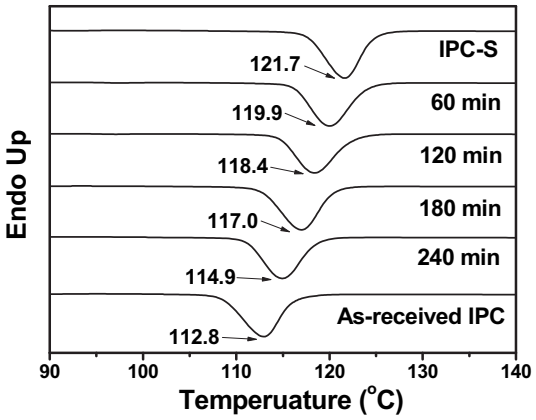

Fig. 2. Crystallization curves of IPC-S after annealing at 200 °C for various durations.

reason for this reversible process has been taken into account that shear could have induced the chain disentanglements which results in the alignments or orientation of PP chains to facilitate the crystallization, and on the other hand, relaxation could occur during thermal annealing. A detailed discussion about this reason is available in the Supplementary Material from which we concluded that the classical shear-induced chain alignments or orientation of PP chains might not be the main reason for the shear-enhanced crystallization in IPC. However, it is more likely that shear promotes the chain disentanglement between iPP and other components causing the breaking of original phase structure, which might help the crystallization of IPC. While in turn, annealing induces a structural motion backwards to achieve re-entanglement and as a result, enhanced crystallization will relax. If phase structure has been varied, the resultant morphology should be readily observed after carefully etching by electron microscopy. Therefore, to testify the above assumptions, we performed an elaborate experiment to demonstrate the possible morphological evolution during melt annealing of IPC-S. We utilized DSC to perform annealing on cryo-fractured IPC-S sample at 200 °C precisely for different time and after which, samples were directly taken out from chamber and quenched to room temperature. The obtained samples were then etched by xylene and coated with gold for subsequent SEM observation.

Fig. 3 displays the SEM micrographs depicting phase morphologies of IPC-S and annealed IPC-S samples. The as-received IPC sample has also been provided for comparison. In Fig. 3 A, IPC-S sample shows no typical phase separated structure with clear boundary as described in previous studies [11,50,51]. Instead, randomly distributed amorphous phases (etched) with irregular dimensions are observed. It seems that pre-shearing procedure has severely damaged the original phase structure of the as-received IPC shown in Fig. 3 F and resulted in a partially miscible system. Analogous shear-induced partial mixing has been reported in PP/EPR system [40], however, the exact nature of this phenomenon is a question that is still open to scientific debate [52]. In IPC system, this shear-induced morphology cannot be stabilized for long at 200 °C as shown in Fig. 3 B that after 60 min annealing, it has evolved to remarkable different phase separated morphology. It shows in Fig. 3 B that the etched phase mainly exhibited a typical bi-continuous morphology, and some small isolated spherical phases could also be observed. With longer annealing, as exhibited in Fig. 3 D and E, it seems that bi-continuous morphology has gradually broken into isolated domain structures. These pictures imply that during the early stage of annealing, spinodal decomposition dominated the phase separation process and induced the bi-continuous morphologies whereas under longer annealing, the appearance of the isolated spherical phases is a natural tendency of the late stages of spinodal

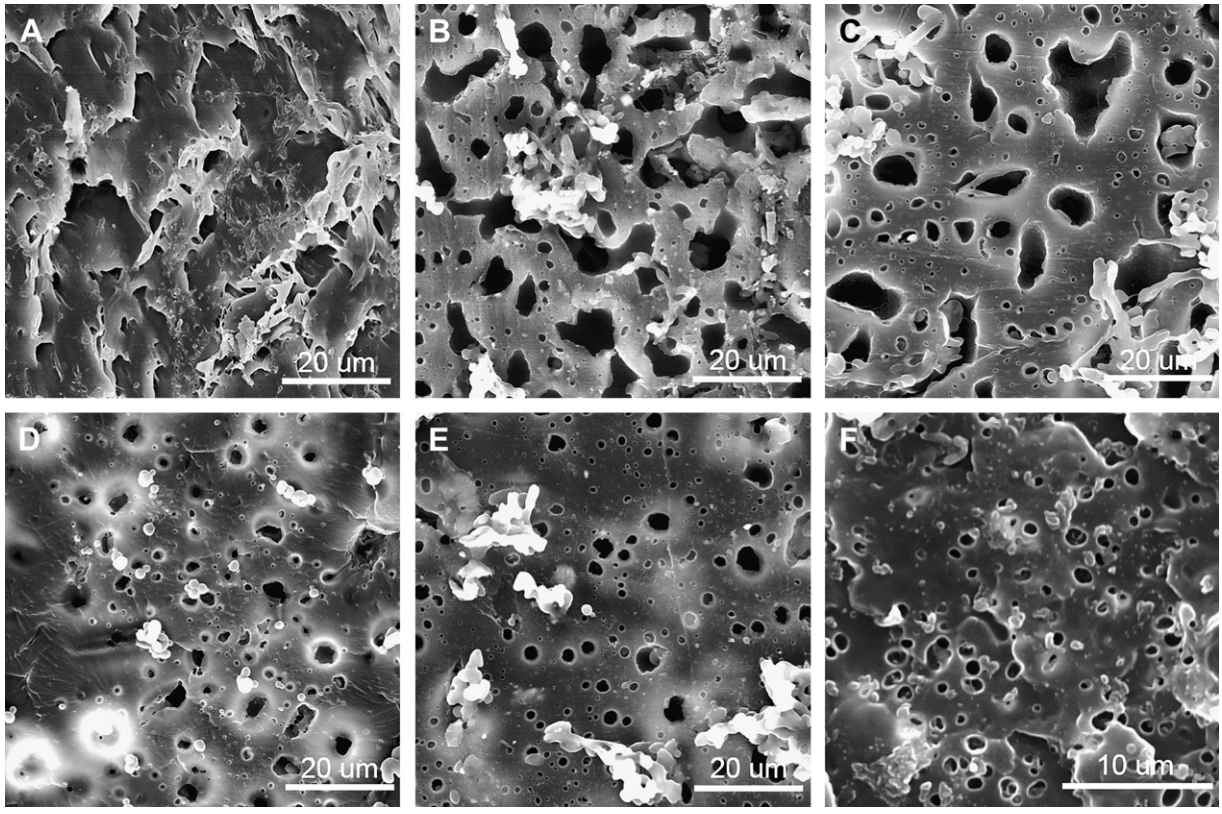

Fig. 3. SEM micrographs of IPC-S (A) and annealed IPC-S after annealing for different durations (B) 60 min (C) 120 min (D) 180 min (E) 240 min and (F) as-received IPC.

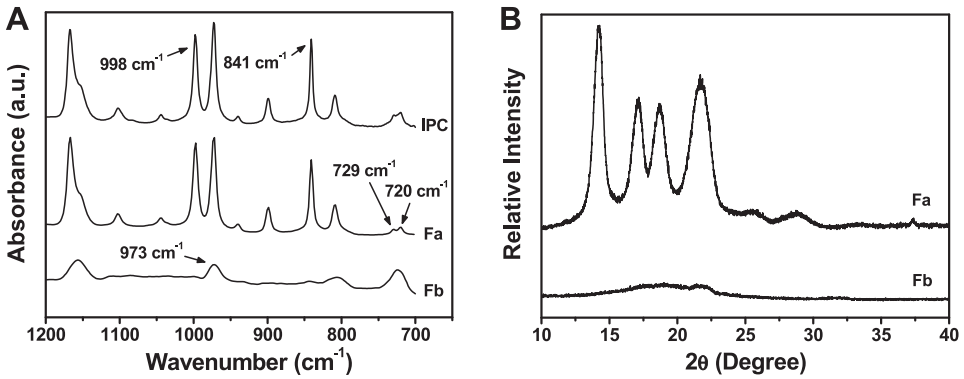

Fig. 4. FTIR (A) characterization of as-received IPC, Fa and Fb, and WAXD (B) scattering curves of Fa and Fb.

decomposition, which might help to reduce the system surface to volume ratio. Because it is hard to precisely measure the extractable phase volume fraction or the sphere diameters concerning the possible local differences and preparation condition, hence, the most convincing information derived from the micrographs is that during annealing, the morphology of IPC-S sample showed a tendency to undergo a spinodal decomposition and transform from bi-continuous to isolated domains with perfectly spherical shape and uniform diameter. Moreover, in Fig. 3 E, it is observed that the fringe areas of some dispersed phases show different contrast compared to the matrix. Earlier studies [14,53] have indicated that during melt annealing, the crystalline EP block copolymers in high impact polypropylene, which shares similar composition with IPC, will enrich and build up the shell of the dispersed phases behaving as the interface-modifier. Hence, we speculate that the different contrast of the fringe area might be related to the formation of such core-shell structure, which helps to the evolvement of amorphous phases and control their shapes and dimensions as observed in the late stage of decomposition. However, it is worth noting that as the SEM cannot discriminate the difference in local composition and also very thin morphological features have a natural tendency to lighten up in SEM, the speculation is not very convincing at the present stage. Whether the core-shell structure exists need further examination by TEM, which will be provided and discussed later in this study. Nevertheless, it should be stressed that the above morphological evolution process can be well correlated to the gradual relaxation of enhanced crystallization in IPC-S, as reflected on the decreasing of T_p shown in Fig. 2.

To sum up, the above results suggested an underlying structural motion during the relaxation of shear-enhanced crystallization. It appears that the phase structure in IPC-S is unstable, and undergoes a morphological evolution upon thermal annealing. Liquid–liquid phase separation approaching the equilibrium state from bi-continuous to isolated spherical domains can be clearly observed. We noticed that during this process, with more stable and regular domain structure formed, the T_p of annealed IPC-S sample decreased indicating a decreasing in crystallization rate. Though the DSC result and SEM micrographs cannot be directly related, we can speculate that an underlying relationship might exist between the two experimental phenomenons at the present stage. Hence, to further clarify the relationship between the varying phase structure and crystallization behavior as suggested, we performed solvent fractionation to destroy and reconstruct the phase structure in IPC, and then characterized its crystallization behavior respectively.

3.3. Crystallization and phase morphology of fractions in IPC

Solvent fractionation performed on IPC has been described in the experimental part. Two characteristic fractions, Fa and Fb, referred to the crystallizable component and amorphous component, respectively, were collected for investigation. Fa corresponds to the component which cannot be dissolved in xylene under room temperature, and Fb corresponds to the soluble component under the same condition. First, FTIR and WAXD characterization methods have been carried out to confirm the phase contents and molecular structures of the two fractions.

The FTIR results of as-received IPC, Fa and Fb are shown in Fig. 4 A. In FTIR spectrums, the absorbance peaks at 998 cm^{-1} and 841 cm^{-1} are the characteristic peaks of crystalline iPP, while the splitted peaks at 729 cm^{-1} and 730 cm^{-1} are attributed to the crystallizable PE sequences. Accordingly, it is evident that fraction Fa is mainly composed of iPP and crystallizable PE components. The crystallizable PE components should include the crystallizable PE segments in either crystalline EP block copolymer, PE segmented polymer or even PE homopolymer as we proposed in our previous study [47]. With regard to fraction Fb, it seems that the peak intensities at 998 cm^{-1} and 841 cm^{-1} are very low. Only one peak at 973 cm^{-1} corresponding to atactic polypropylene and another peak at 720 cm^{-1} corresponding to ethylene segments with very low crystallinity can be observed. Hence, the fraction Fb mainly contains amorphous EPR. The results of WAXD characterization of Fa and Fb, as presented in Fig. 4 B, are quite consistent with the information obtained by FTIR. Fraction Fa exhibits several strong diffraction peaks which correspond to the crystalline polypropylene and polyethylene, indicating a high crystallinity of Fa. Comparatively, fraction Fb only shows a broad peak with very low intensity, which means Fb should be mainly composed of nearly amorphous components. There results proved that the solvent fractionation has successfully separated the crystalline component and amorphous component as we expected.

After clarifying the phase content and molecular structure, the crystallization of the two fractions was studied. The crystallization curves of Fa and Fb derived from DSC measurement are shown in Fig. 5, and the crystallization curve of as-received IPC is also provided for comparison. The crystallization curve of Fb shows two crystallization peaks with very weak intensities at 44.0 °C and 112.4 °C. By comparison with as-received IPC, the crystallization peak at 112.4 °C can be attributed to the crystallization of PP with low molecular weight and isotacticity. On the other hand, the appearance of crystallization peak at 44.0 °C indicates the presence of very short PE segments. As DSC measurements can only detect the crystallizable polymer, the above results proved that except for the amorphous EPR, Fb also contains some components with very low crystallinity (e.g., PP with very low isotacity or short PE segments). However, as the integrated crystallinity of these components is lower than one percent, their existences cannot be detected by WAXD measurement. With respect to fraction Fa, the

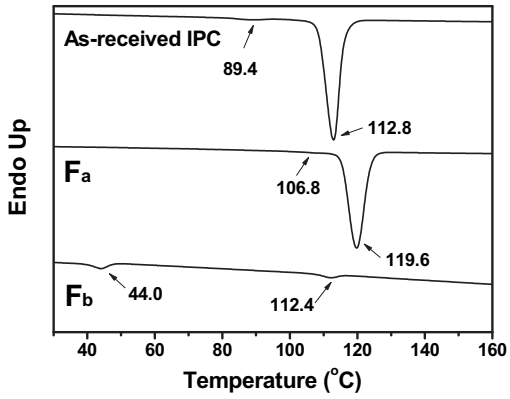

Fig. 5. Crystallization curves of Fa, Fb and as-received IPC.

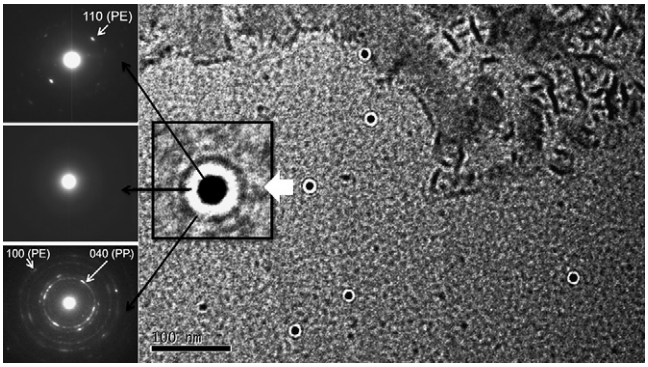

Fig. 6. FETEM graphics of solution casted as-received IPC film with inset of a magnified particle showing multi-layered phase structure. The corresponding SAED patterns are also provided.

crystallization curve shows two peaks, a major one at 119.6 °C and a weak one at 106.8 °C. As the results of FTIR and WAXD exhibited in Fig. 4 have indicated that the major crystalline components in Fa are iPP and crystallizable PE components, it is reasonable to speculate that the major peak can be treated as the crystallization of iPP matrix while the weak peak can be regarded as the crystalline PE. Nevertheless, it is worth mentioning again that the assignment of the two peaks here is only a speculation because no solid proof is available so far. Solvent fractionation and subsequent characterization results has confirmed the complexity of composition and chain structure in IPC. That is, in addition to the main components of crystalline iPP and amorphous EPR, there also exist crystalline polymers with crystallizable PE segments.

However, it is worth noting that in Fa, the T_p of iPP component has increased to 119.6 °C. This elevation of T_p reminded us of the crystallization behavior of IPC-S because two samples exhibited similar enhanced crystallization behaviors. In other words, after removing Fb from IPC, the sample will also show a faster crystallization rate. As we have speculated in Section 3.2, different crystallization behaviors may closely related to the phase structures. Therefore, in order to understand this relationship, the detailed phase structure of the fractions as well as the as-received IPC should be examined.

According to recent studies [13,14], phase structure of IPC can be directly observed by TEM, and different compositions can also be distinguished because of their different contrast induced by density variation. We first observed the original phase structure of as-received IPC. Through solution casting, a thin film of IPC was formed on the pre-heated copper grids. However, the dissolving procedure will certainly alter the original state of the as-received samples. Therefore, after the IPC film was obtained, we have applied certain thermal treatment to this film. The thermal treatment was similar to that applied to the IPC-S that the samples were annealed at 200 °C for about 2 h and then quenched to room temperature using DSC, the purpose of which is to erase the effect of solution casting and exhibit the properties of bulk IPC film. FETEM micrograph of IPC solution casting film is exhibited in Fig. 6, and the inset shows a magnified image of a particle. Many particles with uniform dimensions of several tens of nanometers can be clearly seen from Fig. 6. From the magnified particle as presented, fine phase morphology of as-received IPC is revealed. It seems that the particles exhibit multi-layered phase structure. To ascertain the composition of each layer, we have provided the SAED result (selective area electron diffraction) as indicated by black arrows in Fig. 6. The SAED pattern of the core dark area with the strongest contrast only shows the characteristic orthorhombic crystal of crystalline PE and hence this area should be composed of crystalline PE. Because it is difficult to differentiate the crystallizable PE segments in crystalline EP copolymer or PE homopolymer, hence it is more precisely to define the components in this area as crystalline PE segmented polymer. The white middle layer, as the SAED showed only diffused circles, can be recognized as the amorphous EPR. When we selected the fringe area with weaker contrast compared to the core area for electron diffraction measurement, both the hexagonal crystal structure of PE and monoclinic crystal structure of PP can be observed. Recent study [54] has pointed out that incorporation of propylene unit into PE crystal lattice will lead to the expansion of the cell and formation of hexagonal phase. Hence, the area should be composed of EP block copolymers with both long crystallizable PE and PP segments. Moreover, part of the EP block copolymers seem to link with the crystalline PP matrix, which indicates that some PP segments, because of their good compatibility with iPP, could crystallize into the matrix. On the other hand, the crystallizable PE segments are more inclined to the EPR domain. Thus, the EP block copolymers can serve as interface-modifier or surfactant to improve the connection between the dispersed domains and matrix as well as to control the morphology.

As for Fa and Fb, their phase structures are shown in Fig. 7. As expected, after solvent fractionation, the fractions exhibited remarkably different morphologies. For fraction Fa, the phase structure in Fig. 7 A shows that many dark spherical particles formed in matrix. The SAED pattern of the core area of these particles provided in Fig. 7 A confirmed that these dark particles in Fa can be attributed to the crystalline PE components. The matrix with lower contrast can then be attributed to the crystalline iPP, according to the characterized composition and phase structure of as-received IPC. The crystalline EP block copolymers are believed to exist between dark particles and matrix, however, due to their similar contrast, it is not easy to distinguish directly from the micrograph. With regard to Fb, as shown in Fig. 7 B, it can be observed that there exist two components, one with weakest contrast which should be attributed to the amorphous EPR, and another with stronger contrast randomly scattered which can be regarded as those components with low crystallinity. By FETEM and SAED, we could again confirm the existence of crystalline PP, PE and amorphous EPR, which helps to prove that the compositional information we derived from FTIR, WAXD and DSC was correct. However, the microscopy picture cannot be directly related to the FTIR, WAXD or DSC result. The purpose of microscopic observation is to show the various phase structures of IPC formed under different compositions.

With the aforementioned structural information and detailed phase structure of Fa, Fb and as-received IPC sample, as we have stated, it is reasonable to speculate that there exists a relationship between the varying phase structure and crystallization behavior in IPC. For as-received IPC, the closely packed multi-layered structure shows that the amorphous EPR domains are located within EP block copolymers and crystalline PE segmented polymers, which indicates

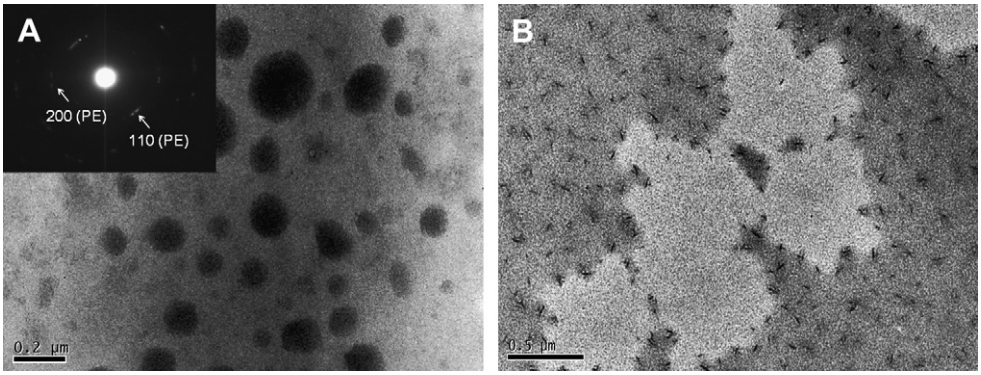

Fig. 7. FETEM graphics of solution casted films of fraction Fa (A) and fraction Fb (B).

a good miscibility between EPR chains and crystallizable PE chains. These chains are highly entangled under the quiescent condition, and as a result, no chances exist for crystallizable PE segments to contact iPP chains in matrix. However, if disentanglement can be achieved through removing EPR from IPC, the original multi-layered structure is no longer existed. Under the circumstance, shearing is no longer a necessity for the crystallization enhancement, as long as the crystallizable PE segments, either in PE segmented polymers or EP block copolymers, are released and have chances to contact PP matrix, for example, by dissolving in solution or by shearing, then the enhanced crystallization could be achieved. Therefore, in fraction Fa where amorphous EPR was removed, we noticed that an enhanced crystallization happened. In brief, it can be concluded that the formation of multi-layered structure and its stability is extremely important to crystallization behaviors in IPC. Under stable state, that is, perfect and closely packed multi-layered structures are formed, the interaction between crystallizable PE segments and iPP matrix is unachievable. Thus, no changing in crystallization can be observed.

According this suggestion, the shear-enhanced crystallization in bulk IPC can also be explained by the following scenario. Under quiescent state, IPC is a phase-separated system forming the multi-layered phase structure. However, shear can destroy this morphology and induce a partially miscibility in IPC implying that a number of the crystallizable PE segments, depending on the condition of shear (see Supplementary Material), could disentangle from EPR and contact iPP matrix, which leads to the acceleration of IPC crystallization. Although both shear and solvent fractionation can destroy the original phase structure, they have remarkable differences in that the destruction by melt shearing is temporary while by solvent fractionation, this destruction is permanent. Therefore, destroyed phase structure in bulk IPC-S, or disentangled chains in other words, can be gradually repaired by melt annealing as observed by the morphological evolution exhibited. Finally, a complete re-entanglement and reconstruction of phase structure can be achieved leading to the vanishing of enhanced crystallization. While for fractioned Fa, it seems only by remixing Fb, the phase structure as well as the crystallization can be recovered backwards.

3.4. Self-assembly of fractions and its influence on crystallization

To further clarify whether varying phase structure in IPC will result in changing of crystallization behavior, we remixed fraction Fa and Fb, and denoted the obtained sample as IPC-R. Fig. 8 A shows the FETEM micrographs of IPC-R solution cast film after annealing at 200 °C for 2 h. The annealing process was still conducted in DSC, the copper grid supporting IPC-R was sealed in an aluminum pan and precisely thermal treated. In Fig. 8 A, an interesting self-assembly of fraction Fa and Fb reflected on the morphological evolution has been observed. Through remixing and annealing, IPC-R sample has spontaneously reformed a perfect multi-layered structure, which is almost the same as that of as-received IPC sample. Some adjacent particles (marked by white arrow) which seem to be separating from each other can also be observed indicating that the IPC-R sample was actually undergoing an evolution towards more stable state. On the other hand, crystallization curve of IPC-R exhibited in Fig. 8 B shows that an obvious recovery of T_p to the lower temperature, which is close to that of as-received IPC sample. It implies that the enhanced crystallization of Fa can be eliminated by remixing with Fb accompanied by reforming the multi-layered structure. Thus, it is again demonstrated the close relationship between the morphological evolution and crystallization in IPC.

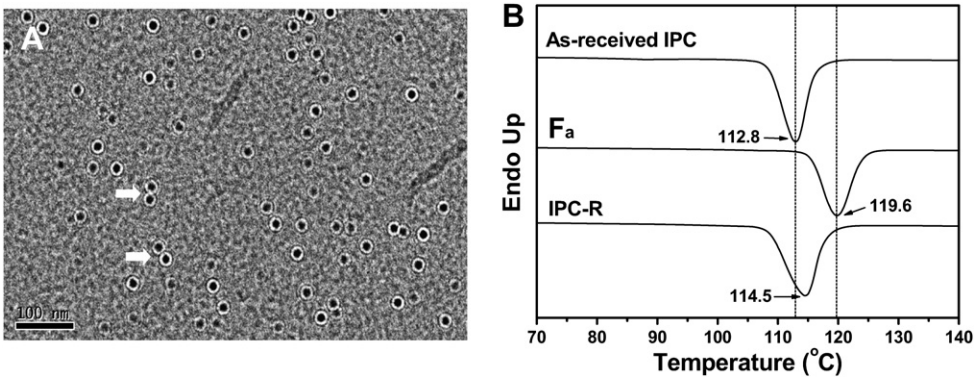

Fig. 8. FETEM graphics of solution casted IPC-R film (A) and crystallization curve of IPC-R (B).

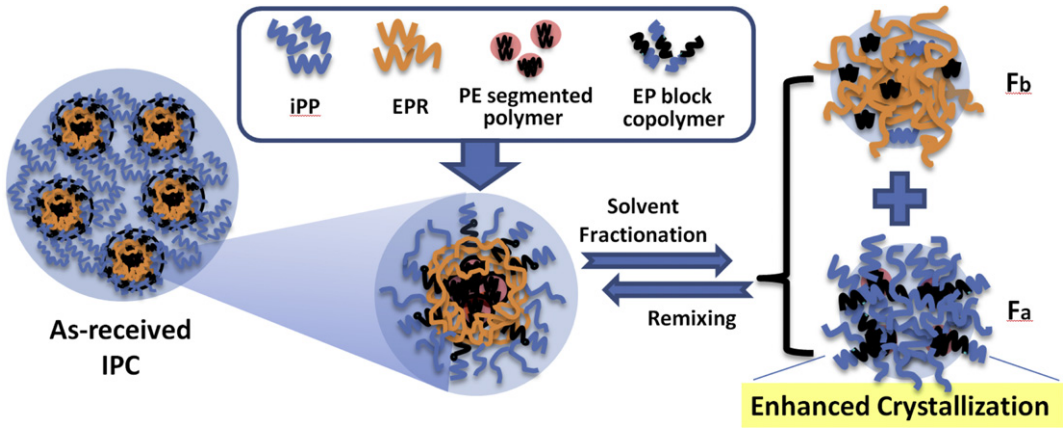

Fig. 9. Schematic model depicting the relationship between phase structure and crystallization behavior in IPC.

On the basis of the above results, we proposed a conceptual model to interpret the phase structure in IPC, and how its evolution will influence the crystallization behavior, as shown in Fig. 9. The four main components in IPC, that is iPP, EPR, EP block copolymer and PE segmented polymer have been marked respectively. Under equilibrium state, the quiescent structure of IPC exhibits a microscopically phase separated morphology. Different components can form a multi-layered structure as shown in the globe left-down in Fig. 9. Because of the existence of EPR as well as the compatibility, the crystallizable PE segments (as indicated by black lines) are confined and separated from iPP matrix. However, by removing EPR, as in the case of Fa, original multi-layered structure will be completely destroyed shown in the globe right-down in Fig. 9. Under the situation, so long as the crystallizable PE segments are released and have chances to contact PP matrix, the enhanced crystallization could be achieved. The possible molecular-scale reason for this faster crystallization may be attributed to the faster nucleation rate of linear PE segments which could serve as stable nuclei to improve the crystallization of iPP. Therefore, overall crystallization behavior will be changed reflected on the enhanced crystallization kinetics. As to the relaxation of enhanced crystallization, if the phase structures are only temporarily destroyed (e.g., shear in bulk), they are hopeful to be gradually repaired under melt annealing, and ultimately recovers to its original state. However, if the destruction of phase structure cannot be recovered, for example removing Fb through solvent fractionation, apparently the crystallization will never be turned back unless the removed fraction is remixed to reconstruct the phase structure.

4. Conclusion

Relaxation of shear-enhanced crystallization in IPC has been investigated from the sight of phase structure and resultant morphological evolution. It is found that melt shearing can destroy the original phase structure of IPC and induce a partial miscibility leading to an enhanced crystallization. The shear-enhanced crystallization in IPC can be gradually eliminated upon melt annealing, and the underlying structural motion is proved to be a reconstruction of phase structure towards equilibrium state. It appears that with sufficient annealing time, IPC-S melt will reform a stable phase structure with domains finely dispersed in the matrix through liquid–liquid phase separation and the enhanced crystallization is likely to be totally eliminated.

By solvent fractionation, FTIR, WAXD, DSC characterizations and FETEM observation, IPC has been proved to be a complex system with multi-component and multiphase nature. It is mainly composed of iPP, EPR, EP block copolymer and PE segmented polymer. Multi-layered phase structure can be observed under stable state and the composition of each layer has been identified. By removing amorphous component out of IPC, multi-layered structure will be destroyed leading to an enhanced crystallization similar to IPC-S. However, by remixing the amorphous component, a morphological evolution through self-assembly of fractions happens, and multi-layered structure can be reformed again. Meanwhile, crystallization behavior recovers back towards the original situation. A model has been proposed to explain the process and it is suggested that in stable multi-layered structure, the crystallizable PE segments are entangled with EPR chains which blocks them from contacting iPP matrix. However, when this structure is destroyed, either by shear or solvent fractionation, the overall crystallization in IPC can be greatly affected.

Acknowledgements

We gratefully acknowledge the financial support from the Natural Science Foundation of China (Grant No. 20874017, 50673021), the National Basic Research Program (G2005CB623803) and the National Hi-Tech Research & Development Program (2007AA03Z450).

Appendix. Supplementary material

Supplementary material associated with this article can be found in the online version, at doi:10.1016/j.polymer.2010.09.008.

References

[1] Galli P, Vecellio G. Prog Polym Sci 2001;26:1287–336.
[2] Simonazzi T, Cecchin G, Mazzullo S. Prog Polym Sci 1991;16:303–29.
[3] Urdampilleta I, Gonzalez A, Iruin JJ, de la Cal JC, Asua JM. Macromolecules 2005;38:2795–801.
[4] Covezzi M, Mei G. Chem Eng Sci 2001;56:4059–67.
[5] Fu ZS, Fan ZQ, Zhang YZ, Xu JT. Polym Int 2004;53:1169–75.
[6] Mirabella FM. Polymer 1993;34:1729–35.
[7] Cai HJ, Luo XL, Ma DZ, Wang JM, Tan HS. J Appl Polym Sci 1999;71:93–101.
[8] Xu JT, Fu ZS, Fan ZQ, Feng LX. Eur Polym J 2002;38:1739–43.
[9] Xu JT, Feng LX, Yang SL, Wu YN, Yang YQ, Kong XM. Polymer 1997;38:4381–5.
[10] Fan YD, Zhang CY, Xue YH, Nie W, Zhang XQ, Ji XL, et al. Polym J 2009;41:1098–104.
[11] Cai HJ, Luo XL, Chen XX, Ma DZ, Wang JM, Tan HS. J Appl Polym Sci 1999;71:103–13.
[12] Chen Y, Chen Y, Chen W, Yang DC. Polymer 2006;47:6808–13.
[13] Chen Y, Chen Y, Chen W, Yang D. J Appl Polym Sci 2008;108:2379–85.
[14] Chen Y, Chen Y, Chen W, Yang D. Eur Polym J 2007;43:2999–3008.
[15] Zhu HJ, Monrabal B, Han CC, Wang DJ. Macromolecules 2008;41:826–33.
[16] Sadler DM, Keller A. Macromolecules 1977;10:1128–40.
[17] Keller A, Sawada S. Makromol Chem 1964;74:190–221.
[18] Hill MJ, Barham PJ, Keller A, Rosney CCA. Polymer 1991;32:1384–93.
[19] Mackley MR, Keller A. Polymer 1973;14:16–20.

[20] Lovinger AJ, Chua JO, Gryte CC. J Polym Sci B Polym Phys Ed 1977;15:641–56.
[21] Lovinger AJ, Williams ML. J Appl Polym Sci 1980;25:1703–13.
[22] Fillon B, Wittmann JC, Lotz B, Thierry A. J Polym Sci B Polym Phys Ed 1993;31:1383–93.
[23] Fillon B, Lotz B, Thierry A, Wittmann JC. J Polym Sci B Polym Phys Ed 1993;31:1395–405.
[24] Lotz B. Polymer 1998;39:4561–7.
[25] Stocker W, Schumacher M, Graff S, Thierry A, Wittmann JC, Lotz B. Macromolecules 1998;31:807–14.
[26] Lotz B. Eur Phys J E 2000;3:185–94.
[27] Lotz B, Cheng SZD. Polymer 2005;46:577–610.
[28] Zhang XQ, Olley RH, Huang BT, Bassett DC. Polym Int 1997;43:45–54.
[29] Dong LS, Olley RH, Bassett DC. J Mater Sci 1998;33:4043–8.
[30] Freedman AM, Bassett DC, Vaughan AS, Olley RH. Polymer 1986;27:1163–9.
[31] Freedman AM, Bassett DC, Olley RH. J Macromol Sci-Phys 1988;B27:319–35.
[32] Hosier IL, Bassett DC, Moneva IT. Polymer 1995;36:4197–202.
[33] Varga J, K-K J. J Polym Sci B Polym Phys Ed 1996;34:657–70.
[34] Hong SM, Seo Y. J Phys Chem B 2007;111:3571–5.
[35] Rathi P, Huang TM, Dayal P, Kyu T. J Phys Chem B 2008;112:6460–6.
[36] Dimeska A, Phillips PJ. Polymer 2006;47:5445–56.
[37] Wang S, Yang DC. Polymer 2004;45:7711–8.
[38] Pang YX, Jia DM, Hu HJ, Hourston DJ, Song M. Polymer 2000;41:357–65.
[39] Leal GP, Asua JM. Polymer 2009;50:68–76.
[40] Lim SW, Lee KH, Lee CH. Polymer 1999;40:2837–44.
[41] Inaba N, Yamada T, Suzuki S, Hashimoto T. Macromolecules 1988;21:407–14.
[42] Chen CY, Yunus W, Chiu HW, Kyu T. Polymer 1997;38:4433–8.
[43] Matsuba G, Shimizu K, Wang H, Wang ZG, Han CC. Polymer 2003;44:7459–65.
[44] Zhang XH, Wang ZG, Muthukumar M, Han CC. Macromol Rapid Commun 2005;26:1285–8.
[45] Zhang XH, Wang ZG, Dong X, Wang DJ, Han CC. J Chem Phys 2006;125:024907.
[46] Wang SJ, Wu CJ, Ren MQ, Van Horn RM, Graham MJ, Han CC, et al. Polymer 2009;50:1025–33.
[47] Song SJ, Feng JC, Wu PY, Yang YL. Macromolecules 2009;42:7067–78.
[48] Song SJ, Wu PY, Feng JC, Ye MX, Yang YL. Polymer 2009;50:286–95.
[49] Shangguan YG, Zhang CH, Xie YL, Chen RF, Jin L, Zheng Q. Polymer 51:500–506.
[50] Tan HS, Li L, Chen ZN, Song YH, Zheng Q. Polymer 2005;46:3522–7.
[51] Yokoyama Y, Ricco T. J Appl Polym Sci 1997;66:1007–14.
[52] Han CC, Yao YH, Zhang RY, Hobbie EK. Polymer 2006;47:3271–86.
[53] Jiang T, Chen HX, Ning YN, Kuang DT, Qu GM. J Appl Polym Sci 2006;101:1386–90.
[54] Du ZX, Xu JT, Dong Q, Fan ZQ. Polymer 2009;50:2510–5.